Am J Stem Cells 2025;14(4):261-276
www.AJSC.us /ISSN:2160-4150/AJSC0167453

Original Article

Analysis of key immune genes in mesenchymal stem cells in a 3D environment

Haojiang Li, Jianfei Gao, Ren Zhang, Jie Liu, Haiquan Tian, Yujia Xin, Xiaoliang Song, Xiangyi Li, Yuewen He

Foot and Ankle Surgery Ward of The Second People's Hospital of Changzhi, No. 82, Heping West Street, Luzhou District, Changzhi 046000, Shanxi, China

Received July 14, 2025; Accepted September 14, 2025; Epub October 15, 2025; Published October 30, 2025

Abstract: Objective: The aim of this study was to identify the different immune-related genes (DIRGs) of mesenchymal stem cells (MSCs) in three-dimensional (3D) vs. two-dimensional (3D) environment. Materials and methods: The gene expression dataset GSE52896 was downloaded from the Gene Expression Omnibus (GEO) database. We obtained immune-related genes from the ImmPort database. The array was processed with the R language to obtain differentially expressed genes (DEGs). A protein-protein interaction (PPI) network was constructed with the STRING database and analyzed with Cytoscape. Gene Ontology (GO) and Kyoto Encyclopedia of Genes and Genomes (KEGG) pathway enrichment analysis data were performed with DAVID (https://davidbioinformatics.nih.gov/). We constructed a least absolute shrinkage and selection operator (LASSO) regression model and multiple support vector machine - recursive feature elimination (mSVM-RFE) model to identify the key DIRGs in cells growing in 3D culture. The performance of the key genes was validated in the GSE58919 dataset. Western blot analysis was performed to verify the expression of one key gene, Cysteine and Glycine Rich Protein 1 (CSRP1). Key immune-related genes were identified using CIBERSORT (https://cibersortx.stanford.edu/). Results: A total of 446 DEGs were screened under two different culture conditions (2D and 3D), and 65 DEGs were identified. GO analysis revealed changes in inflammatory response, extracellular region, and protein binding. KEGG enrichment analysis showed that the DEGs were enriched in pathways involved in cytokine-cytokine receptor interactions, viral protein interactions with cytokines and cytokine receptors and the TNF signaling pathway. Seven key genes were obtained from the intersection of the outputs of the LASSO and mSVM-RFE algorithms. The expression of the seven key genes was verified in the GSE52896 dataset. Western blot (WB) confirmed the alteration of CSRP1 expression under different culture conditions. Conclusion: Stem cells showed significant changes in immune response gene expression under 3D culture conditions. CSRP1 plays essential roles in MSC immunomodulation.

Keywords: 3D culture, MSCs, immunomodulatory, R language, DIRGs, GEO, DEGs, PPI, GO, KEGG, LASSO regression model, mSVM-RFE model, CSRP1

Introduction

Various studies have demonstrated that MSCs are strongly immunosuppressive both in vitro and in vivo. MSCs secrete a broad spectrum of soluble factors that alter the local environment by promoting angiogenesis, tissue repair, cell protection, natural cell growth and inflammation remission [1]. In addition to the repair function of MSCs in the inflammatory environment, increasing evidence indicates that MSCs have potent immunomodulatory effects. Unstimulated MSCs are not immunosuppressive, but when they are the supernatants of activated lymphocytes or stimulated with a combination of IFN-γ and TNF-α, IL-1α or IL-1β, they exert effective immunomodulatory effects. These observations suggest that in some cases, MSCs can acquire an immunosuppressive capacity upon stimulation with inflammatory cytokines [2-4].

According to the existing evidence, MSCs can be considered promising treatment options for refractory inflammatory diseases and immune-related diseases because of their immunomodulatory effects [5, 6]. Immunomodulation by MSCs involves interactions with innate and adaptive immunity, mainly through direct cell-cell contact with immune cells and the paracrine activity of the secretome, such as cytokines, chemokines, growth factors, and other

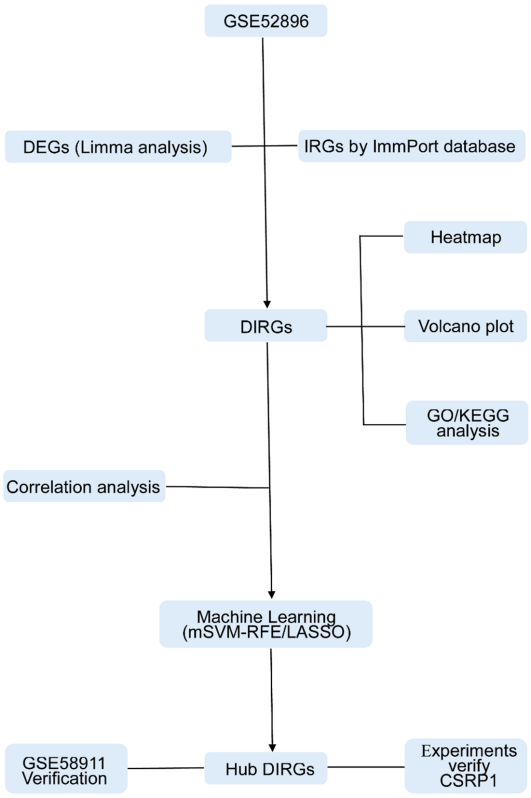

Figure 1. Flowchart showing the research methods used in this study, including searches for DEGs/DIRGs, PPI network construction, enrichment analysis, correlation analysis, machine learning, and DIRG validation.

impactful factors. MSCs can suppress proliferation, interfere with cytotoxicity, and inhibit the secretion of proinflammatory cytokines by NK cells [7]. The underlying mechanisms by which MSCs modulate B cells remain elusive, but various in vitro experiments have confirmed that MSCs can suppress the proliferation, maturation, and antibody production of B cells to a certain extent [8, 9]. Recent studies have shown that MSCs can suppress T cells through direct cell-to-cell contact or the secretion of soluble cytokines. MSCs can suppress the proliferation and activation of CD4+ T cells, CD8+ T cells and Tregs [10, 11]. MSC-induced tolerant DCs can exert immunosuppressive effects [12, 13]. However, the specific mechanism of MSC-induced immunosuppression still requires further exploration.

The immunosuppressive effects of MSCs are utilized in tissue engineering. Most tissue engineering methods involve the cultivation of MSCs on three-dimensional (3D) scaffolds that provide a temporary support structure that mimics the natural shape of living tissue [14-17]. However, the implantation of a stent as a foreign body can cause host rejection, interfere with biological properties, and impair wound healing and tissue remodeling [18-20]. This inflammatory response is characterized by the presence of monocytes, macrophages and giant cells at the interfaces of tissue materials [21-23]. In vivo, the living environment of cells is surrounded by an extracellular matrix (ECM), which provides cell support, mechanical integrity and biological signaling [24]. Natural ECM has a unique 3D structure, ranging from submillimeter to nanoscale fibers and pores [25-27]. In accordance with the structural characteristics of the natural ECM, a stent with a 3D structure can be developed. In previous studies, a significant difference in the immune cell response was detected when the 2D structure was compared to the “natural” 3D microenvironment [28-33].

A study of the potential molecular mechanism underlying the biological behavior of MSCs under different culture conditions, namely, 2D and 3D conditions, with subsequent improvement of the living environment of MSCs is necessary. We explored the molecular mechanisms of immunomodulation between MSCs and different culture environments. A summary of the research methods used in this study is shown in **Figure 1**.

Materials and methods

Array data

The keywords “MSC”, “2D”, and “3D” were used to search the GEO database. The gene expression profiles of MSCs in 2D and 3D culture (GSE 52896) were obtained. The GSE52896 dataset contained 5 MSC samples in 2D culture and 5 MSC samples in 3D culture. The platform for SE52896 was the GLP570 Affymetrix Human Genome U133 Plus 2.0 Array. The platform and series matrix files were all TXT files. The R package was used to process downloaded files and reject unqualified data. The quality of the microarray was evaluated. The data were calibrated and subjected to RMA normalization and log2 conversion, and the KNN method was used to account for missing values. The IRG data were downloaded from the ImmPort database (https://www.immport.org/shared/).

Screen for DEGs and DIRGs

The downloaded files were converted using the R language and annotation packages. The ID corresponding to the probe name was replaced with the international standard name (gene symbol) of the gene. The differential gene expression analysis was performed using the limma package (http://www.bioconductor.org/). The relevant operational instruction code was placed in R, and the limma package was used to analyze the DEGs in the MSC samples in 2D and 3D culture from the microarray dataset. Samples with a *P* value < 0.05 and log fold change (FC) > 1 were considered DEGs. Afterward, 446 DEGs and 1793 IRGs were intersected to obtain 65 differentially expressed immune-related genes (DIRGs).

PPI network construction and analysis

A protein-protein interaction (PPI) network was constructed to explore the interactions between DEGs (https://string-db.org/). A combination score > 0.4 was set as the cutoff standard. Then, Cytoscape was used to visualize the PPI network, and the connections between the nodes represented the interactions among these biomolecules, which could be used to identify proteins encoded by the DEGs in 2D and 3D MSC cultures. The interactions and relationships among the pathways were assessed. We selected the top 10 genes based on the degree value as hub genes.

GO and KEGG enrichment analyses of DIRGs from 3D MSC cultures

Gene Ontology (GO) analysis is a method for annotating genes and identifying characteristic biological attributes from high-throughput genome or transcriptome data. KEGG is a database for the systematic analysis of pathways that links genomic information with functional information. The DAVID database is an online software used to analyze gene functions. Functional and pathway enrichment analyses of the proteins encoded by the candidate genes were performed, and these genes were analyzed using the DAVID database (https://david-bioinformatics.nih.gov/) [34].

The DIRGs obtained from the intersection of DEGs and IRGs were entered into the DAVID online database, with the official gene symbol as the gene set format, *Homo sapiens* as the species, and gene list as the list type. GO enrichment operations can be performed on DIRGs through DAVID online software. $P < 0.05$ was considered to indicate statistical significance.

Using machine learning to construct an IRG prediction model

The least absolute shrinkage and selection operator (LASSO) and multiple support vector machine - recursive feature elimination (mSVM-RFE) algorithms were used to identify key genes in 3D cultured MSCs. In this section, we used R studio and online analysis software for the LASSO and mSVM-RFE algorithms. LASSO is a regression analysis algorithm used to filter variables. In our study, the LASSO algorithm was used via online software (fast.statsape.com). RFE is a selection method that starts with all features and then removes the least important features based on the model's performance. Cross-validation techniques were used to evaluate the performance of the model. The RFE method provides feature ranking based on the importance of features, and top-level features can be selected to construct the final model. Finally, we compared the results of the two regression analyses to obtain key genes related to MSCs in 3D culture.

Experimental verification of DIRGs

A 3D culture environment constructed through 3D printing with a low-temperature deposition technique was constructed using polycaprolactone (PCL). Protein was extracted from cell lysates prepared using RIPA lysis buffer supplemented with a protease inhibitor. Western blot analysis: The amount of protein was determined using a BCA kit. Equal amounts of denatured protein were separated using SDS - PAGE and PVDF membranes. The following primary antibodies were used at a 1:1000 dilution. The membranes were incubated with an HRP-conjugated secondary antibody. The results were detected by a Prime Western blotting Detection System.

Immune cell infiltration in 3D culture of MSCs

We used CIBERSORT, which is based on linear support vector regression (SVR), as an analytical tool for estimating immune cell abundance in 3D MSC culture. CIBERSORT has been used in many tumor-related and other studies. A total

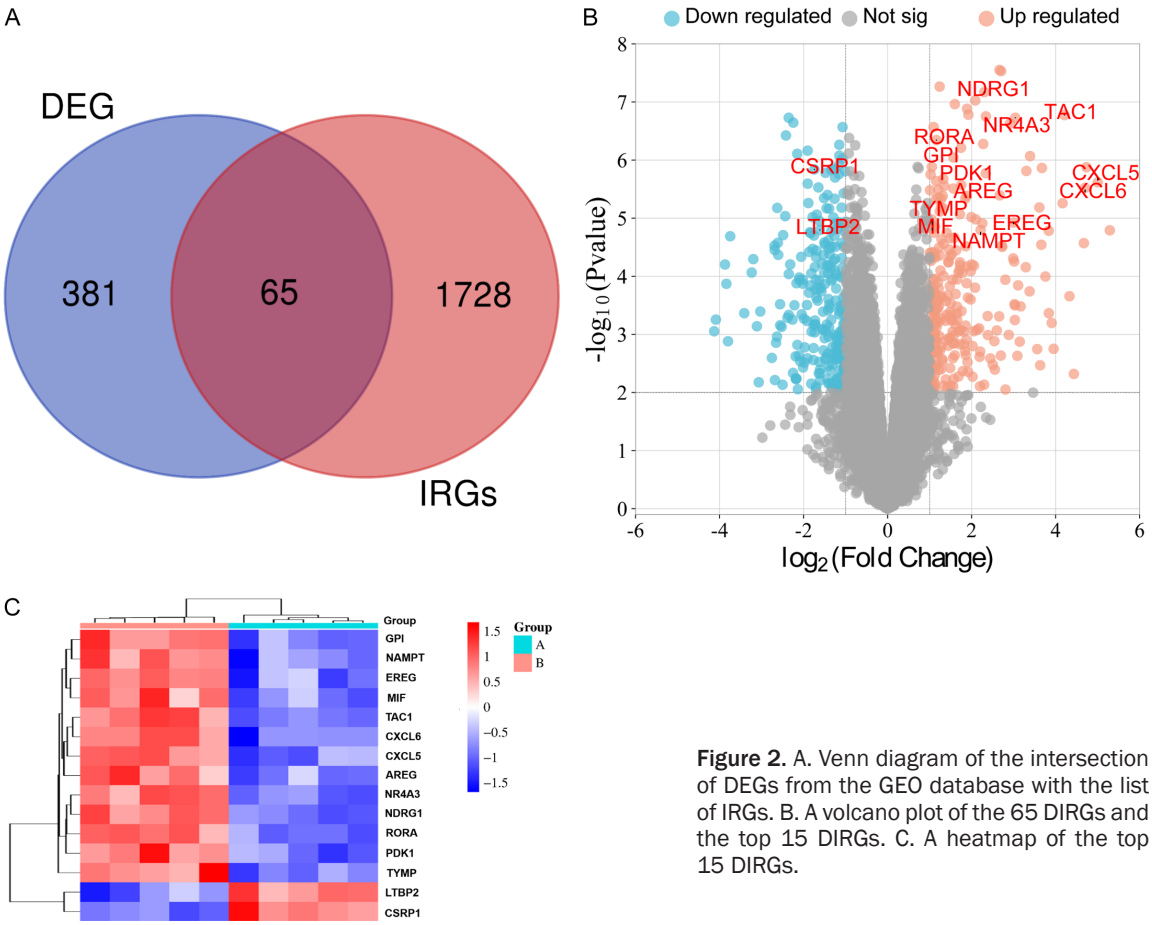

Figure 2. A. Venn diagram of the intersection of DEGs from the GEO database with the list of IRGs. B. A volcano plot of the 65 DIRGs and the top 15 DIRGs. C. A heatmap of the top 15 DIRGs.

of 22 immune cells were compared between the 2D and 3D culture groups.

Statistics

The "limma" package and the "ggplot2" package in R were applied to filter results from the GEO database. The "tidyverse" R package was used to analyze the correlations of DIRGs. The "glmnet" package and "e1071" R package were used in analyses with the LASSO algorithm and the mSVM-RFE algorithm, respectively. The relative expression levels of genes are presented as the means and standard deviations. Student's t test was used for group comparisons. All statistical hypothesis tests were 2-sided and performed at the 0.05 significance level.

Results

Identification of DEGs and DIRGs in 3D culture environments

The microarray dataset GSE52896 containing information on gene expression in MSCs in 3D and 2D environments was preprocessed. Using the limma package (corrected *P* value < 0.05, |log2 FC| > 1), 446 DEGs were obtained, including 237 upregulated genes and 209 downregulated genes were identified. Sixty-five DIRGs were obtained from the intersection of 446 DEGs and 1793 IRGs (**Figure 2A**). We constructed a volcano plot to visualize the IRGs, and the top 15 DIRGs are marked in the chart (**Figure 2B**). The top 15 DIRGs with *P* values < 0.05 and |log2 FC| > 1 are presented in the heatmap (**Figure 2C**). The expression of CSPP1 and LTBP2 was significantly lower in the 3D culture group than that in the 2D culture group. The expression of GPI, NAMPT, MIF, EREG, TAC1, CXCL5, CXCL6, AREG, NR4A3, NDRG1, RORA, PDK1 and TYMP was higher in the 2D culture group than in the 3D culture group.

PPI network and GO/KEGG enrichment analysis

The PPI network was constructed with STRING (http://string.embl.de/) [35] and Cytoscape (version 3.4.0) [36]. PPI networks were con-

structed with proteins with interaction scores > 0.4. A total of 65 DIRGs were selected. In this figure, red indicates upregulated DIRGs, and blue indicates downregulated DIRGs. CXCL8, CXCL12, CXCL1, PTGS2, VCAM1, CCL20, CXCL2, NFKBIA, and TLR2 were the top 10 nodes (**Figure 3A**). The DAVID analysis tool was used to identify biological annotations of the DIRGs in a 3D culture environment and to obtain enriched GO/KEGG terms or pathways. Moreover, the R language, including the "ggplot2" package, was used to visualize the enrichment results. The bubble chart shows the enrichment of the DEGs in the molecular function (MF), biological process (BP) and cell component (CC) categories. In the BP group, the 65 DIRGs were enriched mainly in the inflammatory response and signal transduction. In the molecular function group, the 65 DIRGs were enriched mainly in protein binding and growth factor activity. In the cellular component group, the 65 DIRGs were enriched mainly in the extracellular region and extracellular space (**Figure 3B-D**). DIRGs identified from 3D environmental gene chips were analyzed using the DAVID database. In the KEGG enrichment analysis, the DIRGs were enriched in cytokine receptor interactions and viral protein interactions with cytokines and cytokine receptors (**Figure 3E**). Only the results for the top 2 pathways in the GO/KEGG cluster analyses are listed. These results showed that most DIRGs were significantly related to inflammation.

Correlations of the DIRGs in the 3D culture environment

We further analyze the correlation of the 65 DIRGs. We used the "tidyverse" package in R to plot the results of the correlation analysis for the 65 DIRGs. The top 9 DIRGs with positive and negative correlations were selected, and a network map was constructed (**Figure 4A**). We subsequently constructed a scatter plot to show the genes with the strongest correlation in MSCs in the 3D culture environment. The results indicated that CSRP1 was negatively correlated with AREG, GPI, TNFAIP3, NFKBIA, BMP5, TAC1, and TYMP but not with LGMN (**Figure 4B-E**). Therefore, we hypothesized that CSRP1 plays an essential role in the growth of MSCs in 3D culture environments.

The seven DIRGs identified using machine learning

In our study, machine learning methods, including the LASSO and SVM-RFE algorithms (**Figure 5A-C**), were used to identify essential DIRGs in MSCs cultured in a 3D environment. We selected 7 DIRGs using the LASSO algorithms (LIMS1, NDRG1, RORA, TYMP, CSRP1, CXCL5, and TAC1) as significant prognostic biomarkers in a 3D culture environment (**Figure 5D**). The LASSO algorithms used 10-fold cross-validation. Moreover, the mSVM-RFE model was used to identify 65 DIRGs. A total of 56 DIRGs were selected. Seven DIRGs (LIMS1, NDRG1, RORA, TYMP, CSRP1, CXCL5, and TAC1) were obtained by taking the intersection of the results from the LASSO and mSVM-RFE algorithms; these 7 DIRGs were called key genes and were used for further experimental verification.

Seven DIRGs validated in GSE58919

Seven key genes were selected from the intersection of the LASSO regression model and the mSVM-RFE model. In the principal component analysis, the genes LIMS1, NDRG1, RORA, TYMP, CSRP1, CXCL5, and TAC1 could clearly distinguish MSCs in 2D and 3D culture environments (**Figure 6A**). Therefore, the 7 key genes have essential functions in the immunomodulatory activity of MSCs in 3D culture environments. The heatmap shows the changes in the expression of 7 key genes (**Figure 6B**). We further validated the results, by downloading GSE58919 from the GEO database. In the GSE52896 dataset, 6 genes, namely, LIMS1, NDRG1, RORA, TYMP, CXCL5, and TAC1, were upregulated in the 3D culture group, whereas CSRP1 was downregulated in the 3D culture group. The results from the GSE58919 dataset, were the same as those from the GSE52896 dataset (**Figure 6C**, **6D**).

Validation of CSRP1

We performed experiments to prove our experimental hypothesis. Seeded MSCs were cultured in PCL scaffolds for 2-3 days, which simulated a 3D culture environment. We used live-cell printers to ensure that the MSCs grew on the scaffold (**Figure 7A**). The live-cell printers, live cells and PCL scaffold were provided by our colleagues Doctor Wang and Doctor Sheng. Proteins isolated from seed cells in PCL scaffolds in 3D culture were used to detect the expression of the central gene CSRP1. The expression levels of the CSRP1 gene were lower in the 3D culture group than in the 2D culture group (**Figure 7B**). We found that the expression levels of this DIRG were consistent with the results of the bioinformatics analysis.

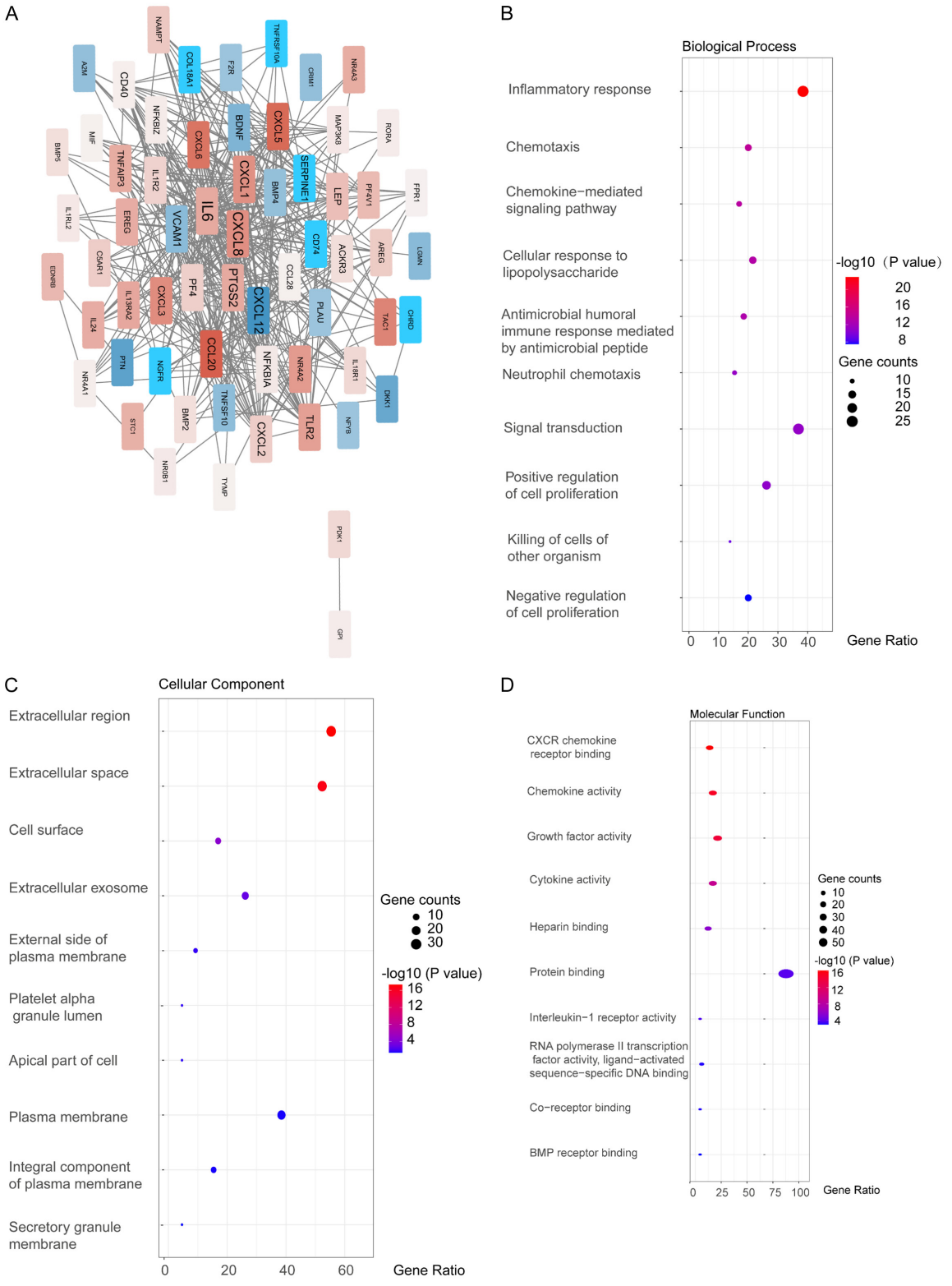
A
NAMPT
COL18A1
F2R
TNFRSF10A
CRIM1
NR4A3
A2M
CD40
NFKBIZ
BDNF
CXCL5
MAP3K6
RORA
MIF
CXCL6
SERPINE1
BMP5
TNFAIP3
IL1R2
CXCL1
BMP4
LEP
PF4V1
FPR1
IL1RL2
EREG
VCAM1
IL6
CXCL8
CD74
ACKR3
AREG
LGMN
C5AR1
EDNRB
PF4
PTGS2
CXCL12
CCL28
PLAU
TAC1
CHRD
IL13RA2
CXCL3
IL24
CCL20
PTN
NGFR
NFKBIA
NR4A2
IL18R1
DKK1
NR4A1
STC1
BMP2
TNFSF10
TLR2
NFYB
CXCL2
NR0B1
TYMP
PDK1
GPI
B
Biological Process
Inflammatory response
Chemotaxis
Chemokine−mediated signaling pathway
Cellular response to lipopolysaccharide
Antimicrobial humoral immune response mediated by antimicrobial peptide
Neutrophil chemotaxis
Signal transduction
Positive regulation of cell proliferation
Killing of cells of other organism
Negative regulation of cell proliferation
0 10 20 30 40
Gene Ratio
-log10 (P value)
20
16
12
8
Gene counts
10
15
20
25
C
Cellular Component
Extracellular region
Extracellular space
Cell surface
Extracellular exosome
External side of plasma membrane
Platelet alpha granule lumen
Apical part of cell
Plasma membrane
Integral component of plasma membrane
Secretory granule membrane
0 20 40 60
Gene Ratio
Gene counts
10
20
30
-log10 (P value)
16
12
8
4
D
Molecular Function
CXCR chemokine receptor binding
Chemokine activity
Growth factor activity
Cytokine activity
Heparin binding
Protein binding
Interleukin−1 receptor activity
RNA polymerase II transcription factor activity, ligand−activated sequence−specific DNA binding
Co−receptor binding
BMP receptor binding
0 25 50 75 100
Gene Ratio
Gene counts
10
20
30
40
50
-log10 (P value)
16
12
8
4

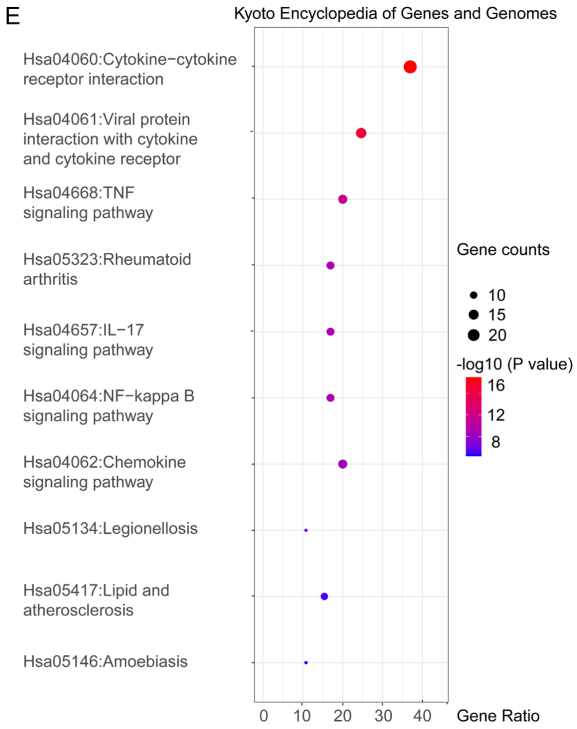

Figure 3. PPI and GO/KEGG analyses. A. The PPI network of 65 DIRGs; red indicates upregulated DIRGs, and blue indicates downregulated DIRGs. B. BP annotations of DIRGs. C. CC annotations of DIRGs. D. MF annotations of DIRGs. E. KEGG annotations of DIRGs.

Distribution of immune cells

We used CIBERSORT to understand the relationships between inflammation and different culture environments. A total of 22 immune-related cells were included in this calculation. Compared with the 2D culture environment, 3D culture of MSCs resulted in a differences in the number of M2 macrophages. We found that the infiltration of M2 macrophages in the 3D culture environment was lower than that of MSCs in 2D culture (**Figure 8**). M2 macrophages are the "healers" of the immune system; M2 macrophages are stimulated by anti-inflammatory cytokines such as IL-4 and IL-13 and play important roles in immunomodulation.

Discussion

In recent years, most studies have improved the understanding of the correlation between MSC tissue engineering and immunomodulation, but few have investigated the potential target genes and molecular mechanisms involved. Furthermore, different MSC culture microenvironments strongly affect the growth and function of MSCs [4]. In this study, 65 DIRGs were screened, 7 of which were identified as key DEGs. We subsequently conducted a series of analyses of the DIRGs, including PPI, GO and KEGG analyses. We further analyzed the correlations of 65 DIRGs and 9 DIRGs. LASSO and mSVM-RFE algorithms were used to identify DIRGs. Seven DIRGs were selected, and we devised a series of experiments to validate our results. Finally, CIBERSORT was used, and the results revealed that M2 macrophages play an important role in the immunomodulatory activity of MSCs.

With the application of stem cells as seed cells in tissue engineering, the immunological characteristics of stem cells are particularly important. Previous experiments have shown that stem cells have low immunogenicity. Moreover, previous experiments in which MSCs derived from human umbilical cord Wharton's jelly (hWJMSC)-scaffold constructs were implanted into rabbits and rats showed that hWJMSCs were present in the animals, with no induction of immune rejection [37]. However, the initial immune microenvironment of MSCs is also particularly important to support the immune immunomodulatory capacity of MSCs. According to some studies of MSCs, the immunomodulatory effect of MSCs on wound healing can be amplified by pretreatment with IFN-γ and TNF-α [38]. Stem cells that were not stimulated to induce activation did not significantly regulate immune activity [2]. In addition, stem

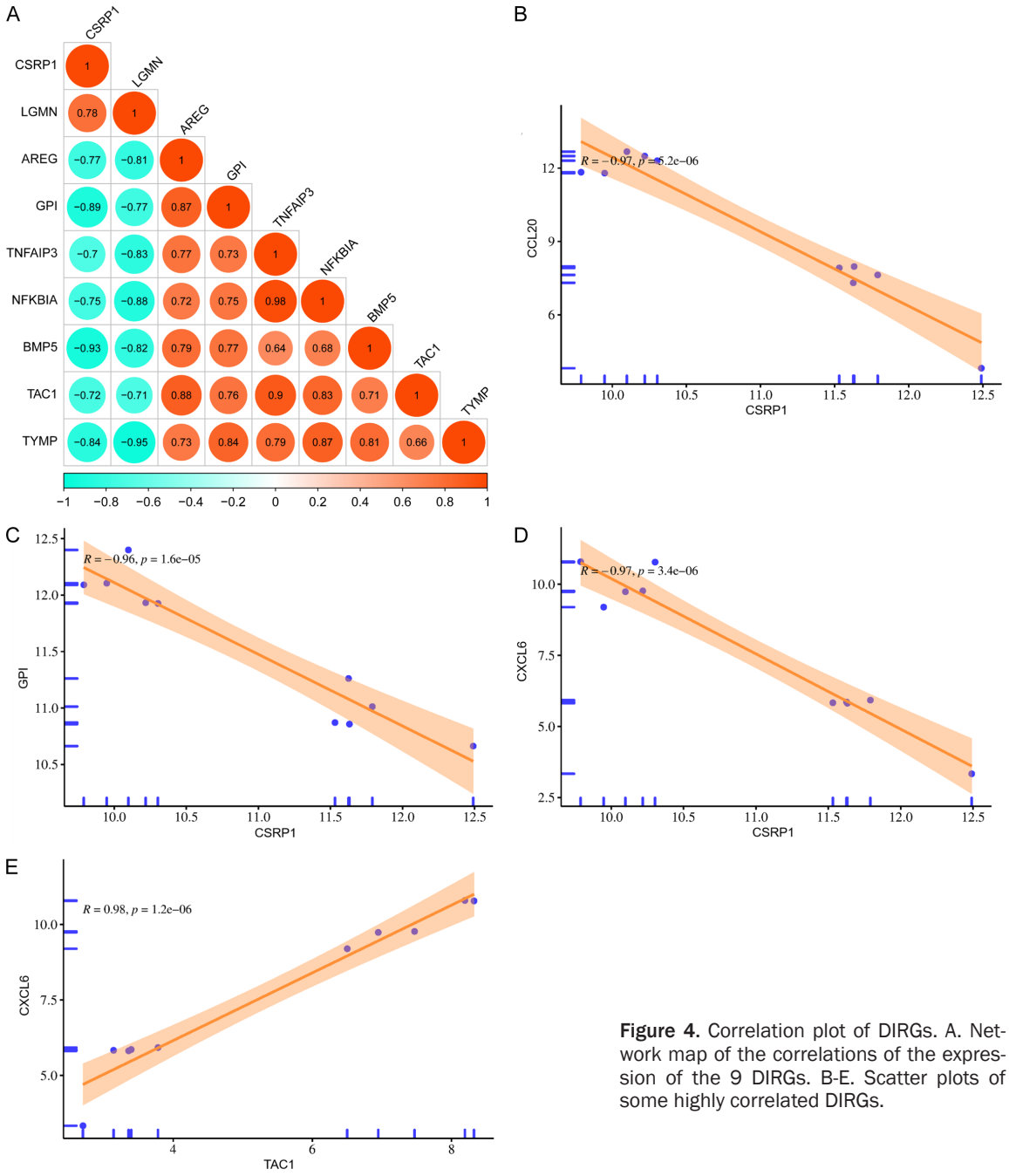

Figure 4. Correlation plot of DIRGs. A. Network map of the correlations of the expression of the 9 DIRGs. B-E. Scatter plots of some highly correlated DIRGs.

cells with differentiation ability, immunophenotypic changes and changes in immunomodulatory capacity during differentiation were also identified in subsequent experiments. The data used in our research were obtained from the GEO online database. R studio was used for data processing, including calibration, normalization and log2 conversion. R studio processing is different from online data processing software, and thus we ensured the quality of the array. The 65 DIRGs were selected through the intersection of the ImmPort database [39, 40] and 446 DEGs, related to immunity.

GO and KEGG enrichment analyses revealed that the TNF signaling pathway, IL-17 signaling pathway, and NF-kappa B signaling pathway are involved in MSC immunomodulation in 3D culture. In a study by Zhuo Chen, IFN-γ and TNF-α synergistically induced PD-L1 expression and

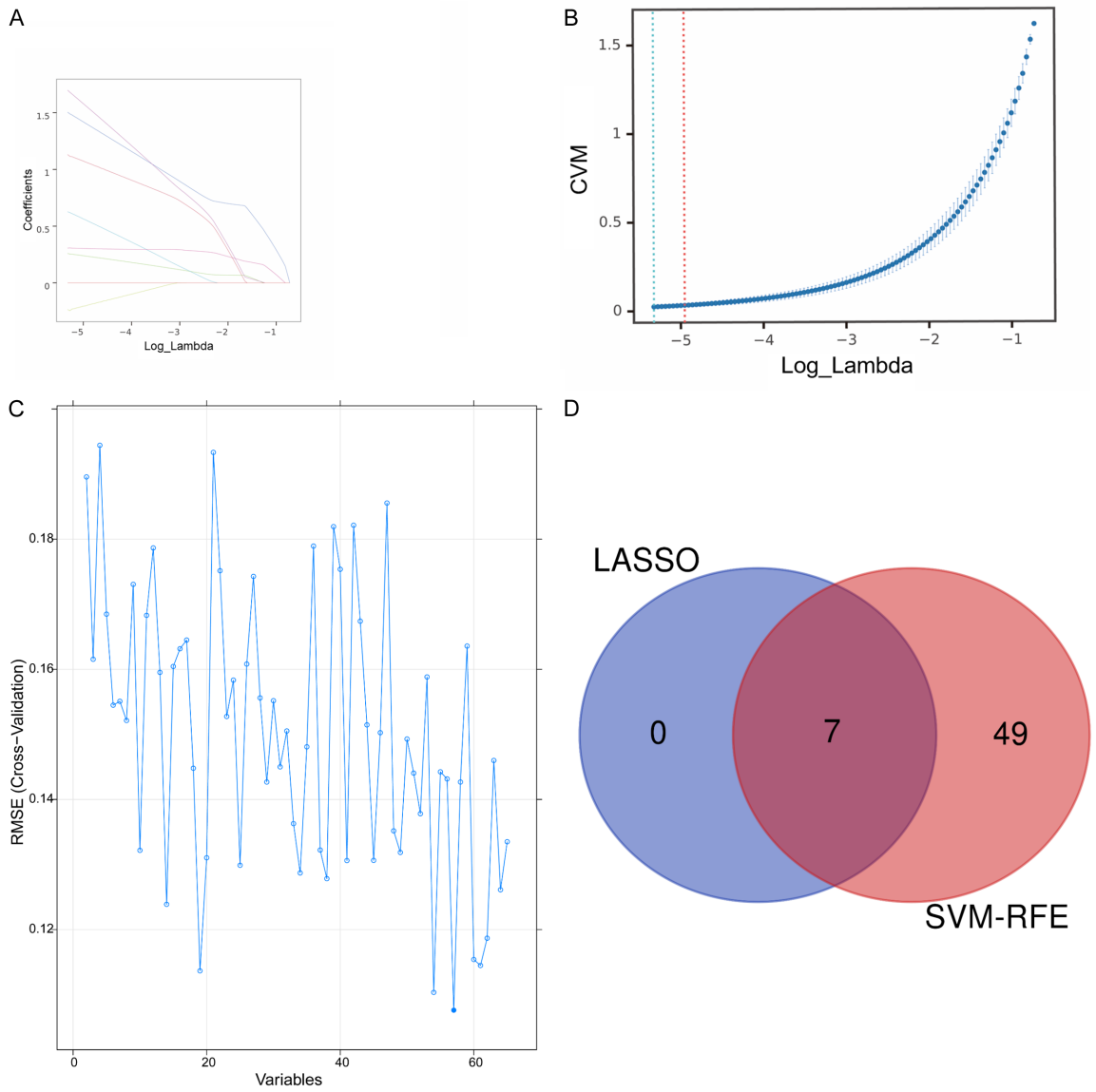

Figure 5. Development of the model. A. LASSO regression coefficient profiles of the 7 DIRGs. Each curve represents the changing trajectory of each DIRG. B. LASSO Cox regression model using partial likelihood deviance versus log(λ). C. Curve of the total within sum of the squared curve under the corresponding cluster number k, which reaches the "elbow point" when k = 56. D. Venn diagram showing the candidate genes that were identified by overlapping the candidate genes selected from the LASSO regression model and the mSVM-RFE model.

enhanced the immunosuppressive capacity of MSCs, and TNF-α significantly increased IFN-γ signaling by activating nuclear factor kappa-B signaling to upregulate IFN-γ receptor expression. IFN-γ activates the JAK/STAT1 signaling pathway, upregulates the expression of the interferon regulator 1 (IRF1) transcription factor, and ultimately promotes the expression of PD-L1 [41]. In a study by Bárbara Du-Rocher, IL-17 did not directly improve MSCs-mediated immunosuppression compared to IFNs, but IL-17 signaling induced the migration of MSCs and inflammatory cells, bringing these cell types in close proximity and increasing the levels of immunosuppressive molecules produced by lymphocyte-sensed MSCs [42].

In addition to the signaling pathways we have identified in the above experiments, previous experimental studies have provided evidence of an association between inflammatory signaling pathways and WNT pathways, suggesting an important mutual concern between the two. Examples of these changes include the upregu-

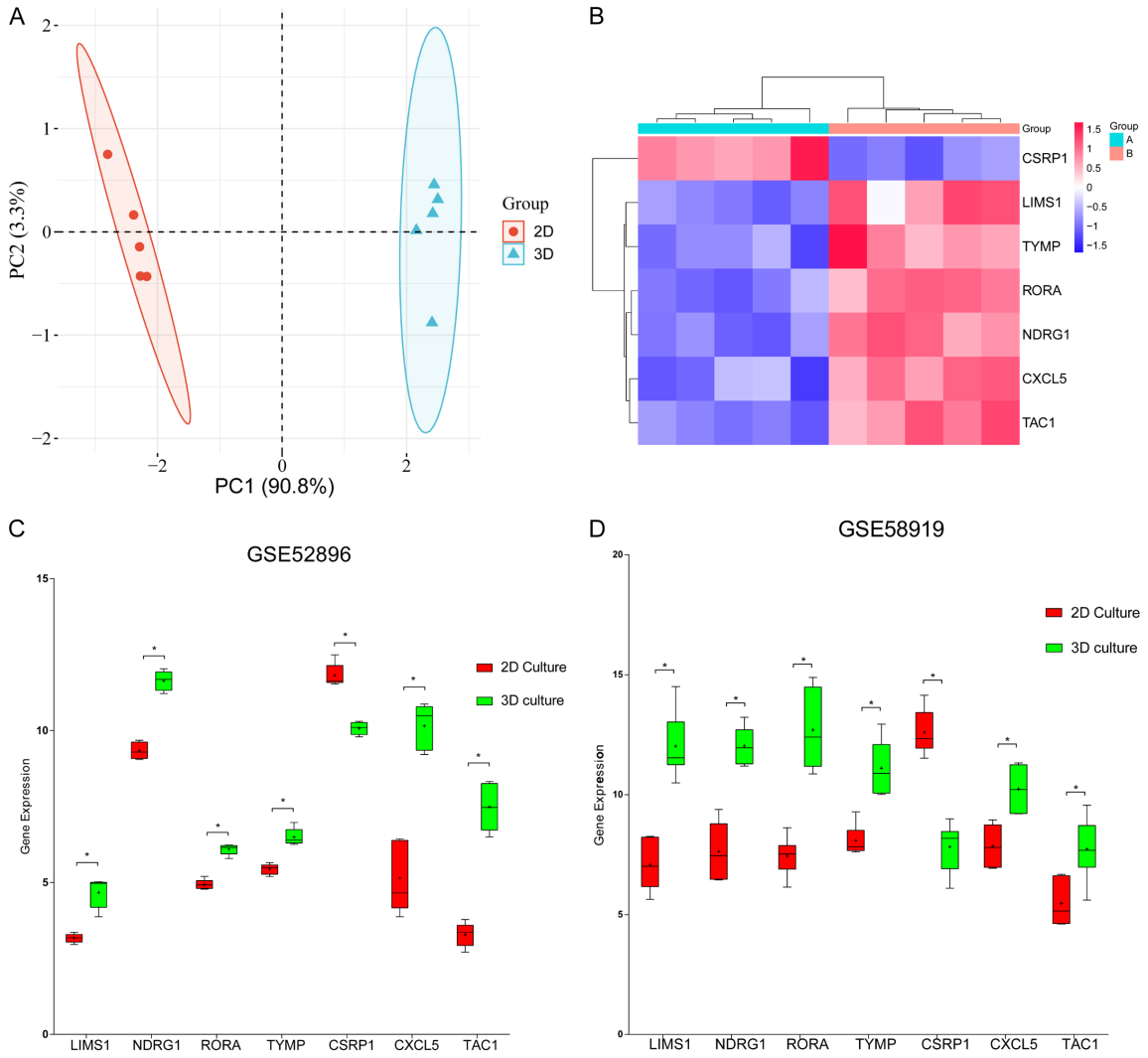

Figure 6. Bioinformatics analysis of 7 DIRGs. (A) Principal component analysis clearly revealed that the 7 genes could clearly distinguish between 2D and 3D cultures. (B) A heatmap of 7 DIRGs. The expression levels of 7 DIRGs between 2D and 3D cultures from the GSE52896 and GSE58919 datasets (C, D).

lation of the secretory activity of the WNT pathway through WNT7b and WNT10a, which regulate macrophage-activated stem cell tissue repair [43].

This study analyzed the expression and regulatory mechanism of DIRGs in MSCs cultured in different environments to further explore the relationship between immunomodulation and 3D culture of MSCs, similar to the predictions reported by Yulin Tao [44-46]. We believe that the techniques chosen should be satisfactory for key genes identified in tissue engineering studies; therefore, the LASSO and mSVM-RFE algorithms were used for identifying key DIRGs. Perhaps the LASSO and mSVM-RFE algorithms are not optimal, and we need to explore new machine learning techniques to validate our conclusions [47]. In the current research on machine learning, differentially expressed genes (DEGs) were screened using weighted gene coexpression network analysis (WGCNA). Five ML algorithms, namely, Bayesian, learning vector quantization (LVQ), wrapper (Boruta), random forest (RF), and logistic regression, were employed to select genes. Seven ML algorithms, including naive Bayes (NB), RF, support vector machine (SVM), AdaBoost classification trees (AdaBoost), boosted logistic regressions (LogitBoost), K-nearest neighbors (KNN), and Cancerclass, were utilized to construct a predictive model [44, 48-50].

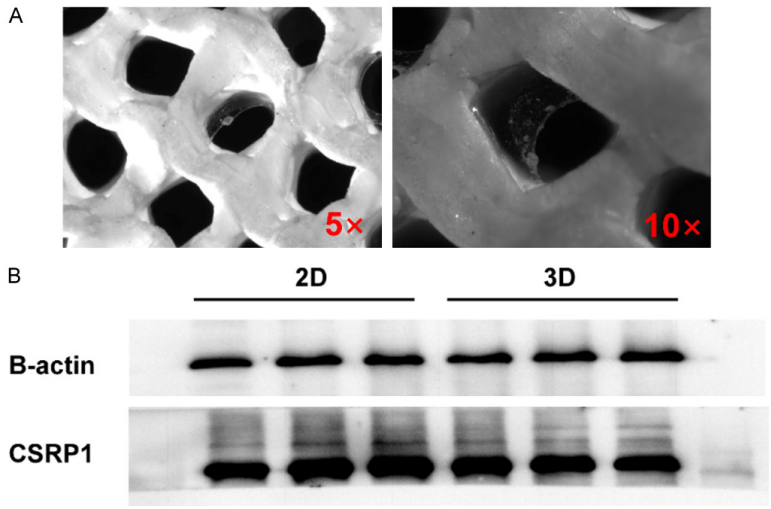

Figure 7. The 3D culture environment constructed using a live-cell 3D printer (A) and WB showing the levels of CSRP1 (B).

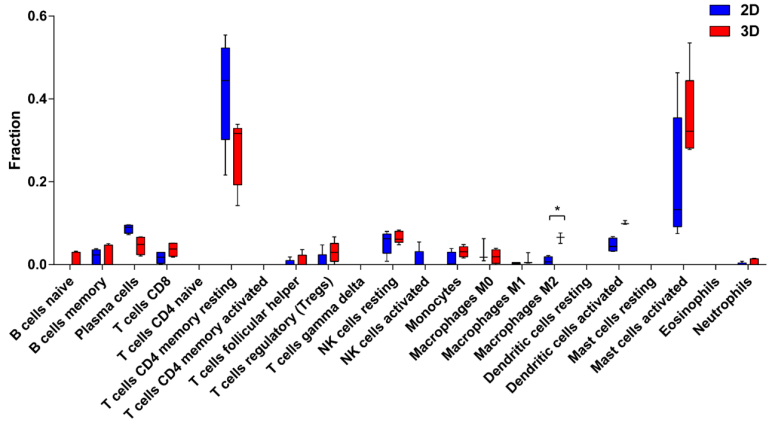

Figure 8. Chart showing the results of the analysis of the infiltration of 22 types of immune cells, where more M2 macrophage infiltrated in 3D cultures than in 2D cultures.

Seven genes (LIMS1, NDRG1, RORA, TYMP, CSRP1, CXCL5, and TAC1) were screened by LASSO regression and mSVM-RFE models in the different culture groups. We verified the expression of LIMS1, NDRG1, RORA, TYMP, CSRP1, CXCL5, and TAC1 by WB. In further experiments, due to sample size limitations, more techniques are needed to explore the molecular mechanism of MSC-mediated immunomodulation. The LIM zinc finger domain containing 1 (LIMS1) gene has been studied in kidney transplant recipients. In a recent study, Krista L. Lentine provided new insights into the pathogenesis of allograft rejection caused by the LIMS1 gene, and suggested that the homozygous deletion of LIMS1 in KTRs may increase the risk of allograft rejection [51]. Krzysztof Kiryluk reported that the LIMS1 locus encodes a minor histocompatibility antigen and is associated with the rejection of the kidney allograft [52]. N-Myc downstream-regulated gene 1 (NDRG-1) is a member of the NDRG family and has important functions in cell differentiation and proliferation. In research by Jianxin Sun, NDRG1 was identified as a key mediator of atherothrombosis and restenosis. NDRG1 may play essential roles in thrombotic responses, and endothelial inflammation. These researchers suggested that NDRG1 inhibition could be a strategy for treating immune-related diseases [53]. Research on NDRG1 has focused on cancer treatment, and this gene is upregulated in bladder cancer, esophageal squamous cell carcinoma, and endometrial, lung and liver cancers but downregulated in colorectal, gastric and ovarian cancers [54]. NDRG1 can inhibit cancer metastasis, but the molecular mechanisms by which NDRG1 inhibits cancer metastasis are still unclear [55]. Retinoic acid receptor-related orphan receptor alpha (RORA), which has been studied by Sarah A Teichmann, is a nuclear receptor that functions as a ligand-dependent transcription factor. According to a previous study, RORA influences the development of Th17 and M2 polarization and plays important roles in skin Tregs [56]. Rora is a negative regulator of the immune system [57]. Thymidine phosphorylase (TYMP), an active driver of endothelial responses, is associated with angiogenesis in tumors, including non-small cell lung cancer, Paget's disease and breast cancer. TYMP can modulate the infiltration of immune cells, such as T cells, Tregs, and mast cells, into tumors. TYMP is upregulated in various cancers [58]. The chemokine CXC motif ligand 5 (CXCL5) is an induc-

ible chemokine that has essential functions in various inflammatory diseases, including cardiovascular disease, DM, and renal disease [60]. Lin Miao reported that CXCL5 is an important chemokine in the tumor microenvironment (TME). The CXCL5/CXCR2 axis can act as a bridge between tumor cells and the TME. CXCL5/CXCR2 inhibitors can increase the effectiveness of immunotherapy and prevent tumor progression [61]. The CXC chemokine system is a component of hypoxia and exerts a strong proinflammatory effect through the activation of hypoxia-inducible factor-1 (HIF-1) and nuclear factor (NF-κB) [62]. Tachykinin 1 (TAC1) belongs to the tachykinin family. Its biological activities are mediated mainly by high-affinity neurokinin 1 receptor (NK-1R), which plays important roles in pain and infectious and inflammatory diseases. Recently, a few reviews of TAC1 have been published. Our recent review revealed that seven immune-related genes play essential roles in MSC immunomodulation, but further study of the underlying molecular mechanism is needed. According to a study by Sheng-Fu Huang, cysteine and glycine-rich protein 1 (CSRP1), a cysteine-rich protein and an immune-related gene, is involved in many cancer-related diseases; these studies have shown that CSRP1 can be used for prediction, but its molecular mechanism and immune cell-related function are unknown [59, 60]. However, in a study by Chunxia Zhao, CSRP1 correlated with immune-related pathways, immune cells, and immune checkpoints. CSRP1 has potential as a novel prognostic factor and appears to influence the immune response in acute myeloid leukemia [63]. Yueji Luo reported that the expression of CSRP1, an immune-related gene, was correlated with the prognosis of kidney renal papillary cell carcinoma and may represent a biomarker for this disease [60].

The immune system is involved in MSC immunomodulation according to CIBERSORT online analysis. The results revealed that 3D-cultured MSCs could polarize macrophages into alternative anti-inflammatory M2 macrophages but not classical proinflammatory M1 macrophages. In a study by Ruijian Yan, PRP hydrogels improved the migration, osteogenic activity and differentiation of MSCs and participated in the immune regulation of the M1-to-M2 transition [64]. In a study by Jun Xiao, PCL hybrid scaffolds promoted osteogenesis and immunomodulation, and M2 macrophages were confirmed to be activated during this process [65]. Guoli Yang reported that hydrogel-based MSC therapy could stimulate M2-polarized macrophage infiltration and facilitate epithelial sealing around implants [66]. In a study by Jing Yang, switching from the M1 phenotype to the M2 phenotype was enhanced by a scaffold carrying dexamethasone, but only by cocultured MSCs [67]. Therefore, MSCs participate in the immunomodulatory 3D culture environment and stimulate the secretion of inflammatory cytokines to regulate cellular immunity. In our research, we rarely detected other immune cells. Therefore, additional bioinformatics data and experiments are needed to confirm our results in future studies. In addition to the effects of MSCs on macrophages, Tregs, B cells, NK cells, neutrophils, DCs, and Th1 or Th17 lymphocytes are all immunomodulated by MSCs, and mesenchymal stem cell-derived extracellular vesicles (MSC-EVs) can modulate the immune response and exhibit immunosuppressive and immunostimulatory properties. However, the immunomodulatory properties of MSCs also promote immune stimulation with a change in the microenvironment.

Finally, our research has several shortcomings. First, the sizes of the GSE52896 and GSE58919 datasets were small. Second, we used only one 3D culture model in our experiments; thus, more 3D cell culture experiments are needed to verify our results. Third, the WB experimental protocol was used separately for the verification of key genes in this study, and therefore, the mutual verification of the results could be achieved through PCR experiments [68]. Finally, the potential immunosuppressive effects on the material or the cells itself needs to be further investigated in future experiments [69].

Conclusion

In our study, we investigated the immunomodulatory activity of MSCs and revealed that immune regulation by MSCs was upregulated in a 3D culture environment. Seven genes, namely, LIMS1, NDRG1, RORA, TYMP, CSRP1, CXCL5, and TAC1, were selected and identified through machine learning. In the final part of our study, we performed WB experiments to verify CSRP1

expression and demonstrate the changes in CSRP1 expression in MSCs under different culture conditions. CIBERSORT was used to validate alterations in M2 macrophages under 3D culture conditions. We propose that these experiments need to be further validated in vivo and in vitro and that a variety of 3D scaffold models require further consideration.

Disclosure of conflict of interest

The authors declare that the research was conducted in the absence of any commercial or financial relationships that could be construed as potential conflicts of interest.

Address correspondence to: Yuewen He, Foot and Ankle Surgery Ward of The Second People's Hospital of Changzhi, No. 82, Heping West Street, Luzhou District, Changzhi 046000, Shanxi, China. E-mail: 15635588186@163.com

References

[1] Wang Y, Fang J, Liu B, Shao C and Shi Y. Reciprocal regulation of mesenchymal stem cells and immune responses. Cell Stem Cell 2022; 29: 1515-1530.

[2] Ren G, Zhang L, Zhao X, Xu G, Zhang Y, Roberts AI, Zhao RC and Shi Y. Mesenchymal stem cell-mediated immunosuppression occurs via concerted action of chemokines and nitric oxide. Cell Stem Cell 2008; 2: 141-150.

[3] Song N, Scholtemeijer M and Shah K. Mesenchymal stem cell immunomodulation: mechanisms and therapeutic potential. Trends Pharmacol Sci 2020; 41: 653-664.

[4] Li H, Shen S, Fu H, Wang Z, Li X, Sui X, Yuan M, Liu S, Wang G and Guo Q. Immunomodulatory functions of mesenchymal stem cells in tissue engineering. Stem Cells Int 2019; 2019: 9671206.

[5] Li Y, Altemus J and Lightner AL. Mesenchymal stem cells and acellular products attenuate murine induced colitis. Stem Cell Res Ther 2020; 11: 515.

[6] Huang Y, Wu Q and Tam PKH. Immunomodulatory mechanisms of mesenchymal stem cells and their potential clinical applications. Int J Mol Sci 2022; 23: 10023.

[7] Moretta A. Natural killer cells and dendritic cells: rendezvous in abused tissues. Nat Rev Immunol 2002; 2: 957-964.

[8] Luz-Crawford P, Djouad F, Toupet K, Bony C, Franquesa M, Hoogduijn MJ, Jorgensen C and Noël D. Mesenchymal stem cell-derived interleukin 1 receptor antagonist promotes macrophage polarization and inhibits b cell differentiation. Stem Cells 2016; 34: 483-492.

[9] Rosado MM, Bernardo ME, Scarsella M, Conforti A, Giorda E, Biagini S, Cascioli S, Rossi F, Guzzo I, Vivarelli M, Dello Strologo L, Emma F, Locatelli F and Carsetti R. Inhibition of B-cell proliferation and antibody production by mesenchymal stromal cells is mediated by T cells. Stem Cells Dev 2015; 24: 93-103.

[10] Ji W, Sun L, Wang D and Zhu W. Mesenchymal stem cells alleviate inflammatory responses through regulation of T-cell subsets. Eur J Pharmacol 2024; 983: 176996.

[11] Li K, Hao Z, Du J, Gao Y, Yang S and Zhou Y. Bacteroides thetaiotaomicron relieves colon inflammation by activating aryl hydrocarbon receptor and modulating CD4(+) T cell homeostasis. Int Immunopharmacol 2021; 90: 107183.

[12] Abbasi-Kenarsari H, Heidari N, Baghaei K, Amani D, Zali MR, Gaffari Khaligh S, Shafiee A and Hashemi SM. Synergistic therapeutic effect of mesenchymal stem cells and tolerogenic dendritic cells in an acute colitis mouse model. Int Immunopharmacol 2020; 88: 107006.

[13] Zhao Y, Su G, Wang Q, Wang R and Zhang M. The CD200/CD200R mechanism in mesenchymal stem cells' regulation of dendritic cells. Am J Transl Res 2021; 13: 9607-9613.

[14] Mallick KK and Cox SC. Biomaterial scaffolds for tissue engineering. Front Biosci (Elite Ed) 2013; 5: 341-360.

[15] Bumroongthai K, Kavanagh DPJ, Genever P and Kalia N. Improving vasculoprotective effects of MSCs in coronary microvessels - benefits of 3D culture, sub-populations and heparin. Front Immunol 2023; 14: 1257497.

[16] Su X, Wang T and Guo S. Applications of 3D printed bone tissue engineering scaffolds in the stem cell field. Regen Ther 2021; 16: 63-72.

[17] SantAnna JPC, Faria RR, Assad IP, Pinheiro CCG, Aiello VD, Albuquerque-Neto C, Bortolussi R, Cestari IA, Maizato MJS, Hernandez AJ, Bueno DF and Fernandes TL. Tissue engineering and cell therapy for cartilage repair: preclinical evaluation methods. Tissue Eng Part C Methods 2022; 28: 73-82.

[18] Anderson JM, Rodriguez A and Chang DT. Foreign body reaction to biomaterials. Semin Immunol 2008; 20: 86-100.

[19] Bryers JD, Giachelli CM and Ratner BD. Engineering biomaterials to integrate and heal: the biocompatibility paradigm shifts. Biotechnol Bioeng 2012; 109: 1898-1911.

[20] Gammon JM and Jewell CM. Engineering immune tolerance with biomaterials. Adv Healthc Mater 2019; 8: e1801419.

[21] Bridges AW, Whitmire RE, Singh N, Templeman KL, Babensee JE, Lyon LA and Garcia AJ. Chronic inflammatory responses to microgel-based implant coatings. J Biomed Mater Res A 2010; 94: 252-258.
[22] Ehashi T, Takemura T, Hanagata N, Minowa T, Kobayashi H, Ishihara K and Yamaoka T. Comprehensive genetic analysis of early host body reactions to the bioactive and bio-inert porous scaffolds. PLoS One 2014; 9: e85132.
[23] Zhang Y, Chen J, Fu H, Kuang S, He F, Zhang M, Shen Z, Qin W, Lin Z and Huang S. Exosomes derived from 3D-cultured MSCs improve therapeutic effects in periodontitis and experimental colitis and restore the Th17 cell/Treg balance in inflamed periodontium. Int J Oral Sci 2021; 13: 43.
[24] Baker BM and Chen CS. Deconstructing the third dimension: how 3D culture microenvironments alter cellular cues. J Cell Sci 2012; 125: 3015-3024.
[25] Park HJ, Yang K, Kim MJ, Jang J, Lee M, Kim DW, Lee H and Cho SW. Bio-inspired oligovitronectin-grafted surface for enhanced self-renewal and long-term maintenance of human pluripotent stem cells under feeder-free conditions. Biomaterials 2015; 50: 127-139.
[26] Samiei M, Alipour M, Khezri K, Saadat YR, Forouhandeh H, Abdolahinia ED, Vahed SZ, Sharifi S and Dizaj SM. Application of collagen and mesenchymal stem cells in regenerative dentistry. Curr Stem Cell Res Ther 2022; 17: 606-620.
[27] Mezey É. Human mesenchymal stem/stromal cells in immune regulation and therapy. Stem Cells Transl Med 2022; 11: 114-134.
[28] Bartneck M, Heffels KH, Pan Y, Bovi M, Zwadlo-Klarwasser G and Groll J. Inducing healing-like human primary macrophage phenotypes by 3D hydrogel coated nanofibres. Biomaterials 2012; 33: 4136-4146.
[29] Bartneck M, Heffels KH, Bovi M, Groll J and Zwadlo-Klarwasser G. The role of substrate morphology for the cytokine release profile of immature human primary macrophages. Mater Sci Eng C Mater Biol Appl 2013; 33: 5109-5114.
[30] Stich S, Stolk M, Girod PP, Thome C, Sittinger M, Ringe J, Seifert M and Hegewald AA. Regenerative and immunogenic characteristics of cultured nucleus pulposus cells from human cervical intervertebral discs. PLoS One 2015; 10: e0126954.
[31] Bou-Ghannam S, Kim K, Grainger DW and Okano T. 3D cell sheet structure augments mesenchymal stem cell cytokine production. Sci Rep 2021; 11: 8170.
[32] Carter K, Lee HJ, Na KS, Fernandes-Cunha GM, Blanco IJ, Djalilian A and Myung D. Characterizing the impact of 2D and 3D culture conditions on the therapeutic effects of human mesenchymal stem cell secretome on corneal wound healing in vitro and ex vivo. Acta Biomater 2019; 99: 247-257.
[33] Pasztorek M, Rossmanith E, Mayr C, Hauser F, Jacak J, Ebner A, Weber V and Fischer MB. Influence of platelet lysate on 2D and 3D amniotic mesenchymal stem cell cultures. Front Bioeng Biotechnol 2019; 7: 338.
[34] Sherman BT, Huang da W, Tan Q, Guo Y, Bour S, Liu D, Stephens R, Baseler MW, Lane HC and Lempicki RA. DAVID Knowledgebase: a gene-centered database integrating heterogeneous gene annotation resources to facilitate high-throughput gene functional analysis. BMC Bioinformatics 2007; 8: 426.
[35] Franceschini A, Szklarczyk D, Frankild S, Kuhn M, Simonovic M, Roth A, Lin J, Minguez P, Bork P, von Mering C and Jensen LJ. STRING v9.1: protein-protein interaction networks, with increased coverage and integration. Nucleic Acids Res 2013; 41: D808-815.
[36] Shannon P, Markiel A, Ozier O, Baliga NS, Wang JT, Ramage D, Amin N, Schwikowski B and Ideker T. Cytoscape: a software environment for integrated models of biomolecular interaction networks. Genome Res 2003; 13: 2498-2504.
[37] Liu S, Yuan M, Hou K, Zhang L, Zheng X, Zhao B, Sui X, Xu W, Lu S and Guo Q. Immune characterization of mesenchymal stem cells in human umbilical cord Wharton's jelly and derived cartilage cells. Cell Immunol 2012; 278: 35-44.
[38] Liu C, Lu Y, Du P, Yang F, Guo P, Tang X, Diao L and Lu G. Mesenchymal stem cells pretreated with proinflammatory cytokines accelerate skin wound healing by promoting macrophages migration and M2 polarization. Regen Ther 2022; 21: 192-200.
[39] Lu Y, Li K, Hu Y and Wang X. Expression of immune related genes and possible regulatory mechanisms in Alzheimer's disease. Front Immunol 2021; 12: 768966.
[40] Yang X, Su X, Wang Z, Yu Y, Wu Z and Zhang D. ULBP2 is a biomarker related to prognosis and immunity in colon cancer. Mol Cell Biochem 2023; 478: 2207-2219.
[41] Chen Z, Yao MW, Shen ZL, Li SD, Xing W, Guo W, Li Z, Wu XF, Ao LQ, Lu WY, Lian QZ, Xu X and Ao X. Interferon-gamma and tumor necrosis factor-alpha synergistically enhance the immunosuppressive capacity of human umbilical-cord-derived mesenchymal stem cells by increasing PD-L1 expression. World J Stem Cells 2023; 15: 787-806.
[42] Du-Rocher B, Binato R, de-Freitas-Junior JCM, Corrêa S, Mencalha AL, Morgado-Díaz JA and

Abdelhay E. IL-17 triggers invasive and migratory properties in human MSCs, while IFNy favors their immunosuppressive capabilities: implications for the "licensing" process. Stem Cell Rev Rep 2020; 16: 1266-1279.
[43] Zhang Q, Yu J, Chen Q, Yan H, Du H and Luo W. Regulation of pathophysiological and tissue regenerative functions of MSCs mediated via the WNT signaling pathway (Review). Mol Med Rep 2021; 24: 648.
[44] Arfat Y, Mittone G, Esposito R, Cantalupo B, DE Ferrari GM and Aldinucci M. Machine learning for cardiology. Minerva Cardiol Angiol 2022; 70: 75-91.
[45] Silva GFS, Fagundes TP, Teixeira BC and Chiavegatto Filho ADP. Machine learning for hypertension prediction: a systematic review. Curr Hypertens Rep 2022; 24: 523-533.
[46] Lee YW, Choi JW and Shin EH. Machine learning model for predicting malaria using clinical information. Comput Biol Med 2021; 129: 104151.
[47] Greener JG, Kandathil SM, Moffat L and Jones DT. A guide to machine learning for biologists. Nat Rev Mol Cell Biol 2022; 23: 40-55.
[48] Tao Y, Xiong M, Peng Y, Yao L, Zhu H, Zhou Q and Ouyang J. Machine learning-based identification and validation of immune-related biomarkers for early diagnosis and targeted therapy in diabetic retinopathy. Gene 2025; 934: 149015.
[49] Sultan AS, Elgharib MA, Tavares T, Jessri M and Basile JR. The use of artificial intelligence, machine learning and deep learning in oncologic histopathology. J Oral Pathol Med 2020; 49: 849-856.
[50] Guo W, Liu J, Dong F, Song M, Li Z, Khan MKH, Patterson TA and Hong H. Review of machine learning and deep learning models for toxicity prediction. Exp Biol Med (Maywood) 2023; 248: 1952-1973.
[51] Caliskan Y, Karahan G, Akgul SU, Mirioglu S, Ozluk Y, Yazici H, Demir E, Dirim AB, Turkmen A, Edwards J, Savran FO, Sever MS, Kiryluk K, Gharavi A and Lentine KL. LIMS1 risk genotype and T cell-mediated rejection in kidney transplant recipients. Nephrol Dial Transplant 2021; 36: 2120-2129.
[52] Steers NJ, Li Y, Drace Z, D'Addario JA, Fischman C, Liu L, Xu K, Na YJ, Neugut YD, Zhang JY, Sterken R, Balderes O, Bradbury D, Ozturk N, Ozay F, Goswami S, Mehl K, Wold J, Jelloul FZ, Rohanizadegan M, Gillies CE, Vasilescu EM, Vlad G, Ko YA, Mohan S, Radhakrishnan J, Cohen DJ, Ratner LE, Scolari F, Susztak K, Sampson MG, Deaglio S, Caliskan Y, Barasch J, Courtney AE, Maxwell AP, McKnight AJ, Ionita-Laza I, Bakker SJL, Snieder H, de Borst MH, D'Agati V, Amoroso A, Gharavi AG and Kiryluk K. Genomic mismatch at LIMS1 locus and kidney allograft rejection. N Engl J Med 2019; 380: 1918-1928.
[53] Zhang G, Qin Q, Zhang C, Sun X, Kazama K, Yi B, Cheng F, Guo ZF and Sun J. NDRG1 signaling is essential for endothelial inflammation and vascular remodeling. Circ Res 2023; 132: 306-319.
[54] Ghafouri-Fard S, Ahmadi Teshnizi S, Hussen BM, Taheri M and Sharifi G. A review on the role of NDRG1 in different cancers. Mol Biol Rep 2023; 50: 6251-6264.
[55] Zhao X and Richardson DR. The role of the NDRG1 in the pathogenesis and treatment of breast cancer. Biochim Biophys Acta Rev Cancer 2023; 1878: 188871.
[56] Walker JA, Clark PA, Crisp A, Barlow JL, Szeto A, Ferreira ACF, Rana BMJ, Jolin HE, Rodriguez-Rodriguez N, Sivasubramaniam M, Pannell R, Cruickshank J, Daly M, Haim-Vilmovsky L, Teichmann SA and McKenzie ANJ. Polychromic reporter mice reveal unappreciated innate lymphoid cell progenitor heterogeneity and elusive ILC3 progenitors in bone marrow. Immunity 2019; 51: 104-118, e107.
[57] Haim-Vilmovsky L, Henriksson J, Walker JA, Miao Z, Natan E, Kar G, Clare S, Barlow JL, Charidemou E, Mamanova L, Chen X, Proserpio V, Pramanik J, Woodhouse S, Protasio AV, Efremova M, Griffin JL, Berriman M, Dougan G, Fisher J, Marioni JC, McKenzie ANJ and Teichmann SA. Mapping Rora expression in resting and activated CD4+ T cells. PLoS One 2021; 16: e0251233.
[58] Chen SA, Zhang JP, Wang N and Chen J. Identifying TYMP as an immune prognostic marker in clear cell renal cell carcinoma. Technol Cancer Res Treat 2023; 22: 15330338231194555.
[59] Zhang ZJ, Huang YP, Liu ZT, Wang YX, Zhou H, Hou KX, Tang JW, Xiong L, Wen Y and Huang SF. Identification of immune related gene signature for predicting prognosis of cholangiocarcinoma patients. Front Immunol 2023; 14: 1028404.
[60] Luo Y, Chen D and Xing XL. Comprehensive analyses revealed eight immune related signatures correlated with aberrant methylations as prognosis and diagnosis biomarkers for kidney renal papillary cell carcinoma. Clin Genitourin Cancer 2023; 21: 537-545.
[61] Zhang W, Wang H, Sun M, Deng X, Wu X, Ma Y, Li M, Shuoa SM, You Q and Miao L. CXCL5/CXCR2 axis in tumor microenvironment as potential diagnostic biomarker and therapeutic target. Cancer Commun (Lond) 2020; 40: 69-80.
[62] Korbecki J, Kojder K, Kapczuk P, Kupnicka P, Gawrońska-Szklarz B, Gutowska I, Chlubek D

and Baranowska-Bosiacka I. The effect of hypoxia on the expression of CXC chemokines and CXC chemokine receptors-a review of literature. Int J Mol Sci 2021; 22: 843.

[63] Zhao C, Wang Y, Wang H, Sharma A, Wu Y, Schmidt-Wolf IGH and Wang Z. CSRP1 gene: a potential novel prognostic marker in acute myeloid leukemia with implications for immune response. Discov Oncol 2024; 15: 248.

[64] Jiang G, Li S, Yu K, He B, Hong J, Xu T, Meng J, Ye C, Chen Y, Shi Z, Feng G, Chen W, Yan S, He Y and Yan R. A 3D-printed PRP-GelMA hydrogel promotes osteochondral regeneration through M2 macrophage polarization in a rabbit model. Acta Biomater 2021; 128: 150-162.

[65] Ji X, Yuan X, Ma L, Bi B, Zhu H, Lei Z, Liu W, Pu H, Jiang J, Jiang X, Zhang Y and Xiao J. Mesenchymal stem cell-loaded thermosensitive hydroxypropyl chitin hydrogel combined with a three-dimensional-printed poly(ε-caprolactone)/nano-hydroxyapatite scaffold to repair bone defects via osteogenesis, angiogenesis and immunomodulation. Theranostics 2020; 10: 725-740.

[66] Li Y, Zhang J, Wang C, Jiang Z, Lai K, Wang Y and Yang G. Porous composite hydrogels with improved MSC survival for robust epithelial sealing around implants and M2 macrophage polarization. Acta Biomater 2023; 157: 108-123.

[67] Majrashi M, Kotowska A, Scurr D, Hicks JM, Ghaemmaghami A and Yang J. Sustained release of dexamethasone from 3D-printed scaffolds modulates macrophage activation and enhances osteogenic differentiation. ACS Appl Mater Interfaces 2023; 15: 56623-56638.

[68] Hao S, Xinqi M, Weicheng X, Shiwei Y, Lumin C, Xiao W, Dong L and Jun H. Identification of key immune genes of osteoporosis based on bioinformatics and machine learning. Front Endocrinol (Lausanne) 2023; 14: 1118886.

[69] Xin L, Lin X, Zhou F, Li C, Wang X, Yu H, Pan Y, Fei H, Ma L and Zhang S. A scaffold laden with mesenchymal stem cell-derived exosomes for promoting endometrium regeneration and fertility restoration through macrophage immunomodulation. Acta Biomater 2020; 113: 252-266.